

# Protection of columns in buildings against accidental impact, fire and progressive collapse

Luiz Eduardo Gonçalves de Mattos<sup>1</sup>, José Caio Couto Bezerra Carneiro<sup>1</sup>, André Teófilo Beck<sup>1</sup>

<sup>1</sup>*Dept. of Structural Engineering, University of São Paulo  
Av Trabalhador São-carlense, 400, 13566-590, São Carlos, SP, Brazil  
luizmattos@usp.br, josecaiocouto@usp.br, atbeck@sc.usp.br*

**Abstract.** Civil structures must be designed to withstand demands throughout their lifespan, ensuring adequate safety levels. However, accidental events, such as fires and vehicular impacts, presents high uncertainty regarding intensity, location and occurrence probability, potentially exposing the structure's lack of robustness and representing significant risk. An accidental column loss, for example, can trigger progressive collapse. To prevent disproportionate damage, reinforcements or protection devices can be used. However, traditional reinforcements can be expensive and impractical, especially in existing buildings. In this context, an optimized structural protection device is proposed for reinforced concrete columns, capable of inhibiting or reducing damage caused by impacts and fires and reducing the likelihood of collapse due to falling slabs. The device consists of cellular structures, known for their energy absorption and thermal insulation properties. A cost-benefit analysis based on risk minimization is also presented, aiming to reduce expected failure costs and failure probabilities in adverse scenarios. Supported by positive results, it is concluded that the cellular protection device is a good alternative to traditional structural reinforcement techniques, standing out for its versatility, effectiveness, and potential for application with reduced costs.

**Keywords:** structural protection device, progressive collapse, risk optimization, reliability analysis

## 1 Introduction

Structural robustness refers to the ability to prevent disproportionately severe damage and exaggerated amplification of initial damage, as highlighted by Melchers and Beck [1]. Preventing progressive collapse has led to the development of standards and techniques, such as the Alternative Path Method (APM), which ensures that adjacent elements are strong enough to prevent the propagation of failure even with localized element loss. Reinforcement techniques are costly and depend on economic feasibility and architectural possibilities. Kiakojoury et al. [2] state that load redistribution measures, like APM, are uneconomical for smaller initial failures, such as column loss.

Beck et al. [3] evaluated the cost-benefit of APM in cases of column loss due to extreme events, indicating that the economic viability of reinforcement is related to the occurrence probability of these hazards.

Local adaptation techniques, such as protective devices for columns against vehicle impacts and flame-retardant materials, are viable alternatives when traditional measures are inadequate.

The probability of global structural collapse, considering multiple hazards, is described by [4]:

$$P[C] = \sum_H \sum_{LD} P[C|LD, H]P[LD|H]P[H]. \quad (1)$$

$P[H]$  is the probability of hazard occurrence,  $P[LD|H]$  is the probability of local damage conditioned on the hazard  $H$ , and  $P[C|LD, H]$  is the probability of global collapse conditioned on local damage and hazard occurrence.

To mitigate the propagation of failure initiated by hazard  $H$ , implementing protective measures and structural reinforcements is essential. Structural robustness controls the probabilities of local damage  $P[LD|H]$  and its spread, thereby reducing the likelihood of global collapse  $P[C|LD, H]$ .

## 2 Cellular structures

The use of cellular structures inspired by honeycomb designs has gained prominence in various applications, including column protection. These structures are renowned for their exceptional energy absorption and thermal insulation properties, as mentioned by Wang [5]. The interconnected cell geometry ensures efficient load distribution, enabling controlled dissipation of impact energy and minimizing damage. Additionally, honeycomb structures act as highly effective thermal insulators due to the presence of trapped air cells within their framework, significantly reducing the effects of thermal conduction and convection.

Hexagonal shapes are conventionally the most used and are manufactured with various materials. However, the search for geometries more suitable for specific applications has driven the evolution and development of research in pursuit of more satisfactory configurations. The protection device proposed in this paper consists of square cellular structures. According to Gibson and Ashby [6], the relative density ( $\rho_r$ ), given by the ratio between the effective density of the cellular structure ( $\rho_e$ ) and the density of the base material ( $\rho_s$ ), is an important parameter for describing and producing honeycomb structures.

### 2.1 Mechanical properties

Comprehensive studies investigate the out-of-plane mechanical behavior of cellular structures to maximize the energy absorption capacity of sandwich panels. The base material, cell shape, and relative density are key factors influencing strength. Analytical models that describe the mechanical properties as functions of relative density, base material properties, and cellular format are proposed by Gibson and Ashby [6].

Figure 1 presents the stress-strain curve of cellular structures under compression, along with a perspective view of a square cellular structure.

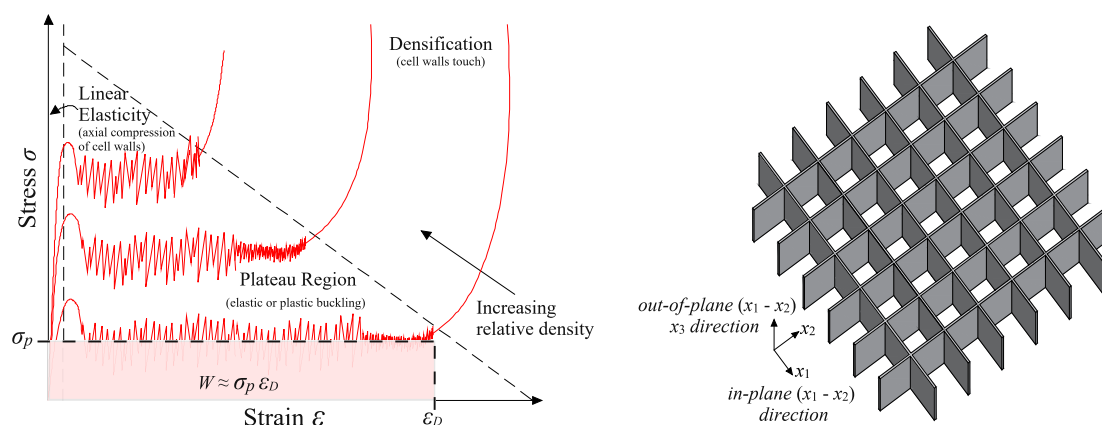


Figure 1. Stress-strain curve and perspective view of a cellular structure.

These structures initially display a linear-elastic regime, followed by a plateau stress ( $\sigma_p$ ) region, and then increasing stresses. Oscillations in the plateau region result from folding in the cell walls. Final failure occurs through rupture or densification ( $\varepsilon_D$ ) when the cell walls touch, with models considering the formation of progressive folds and additional plastic hinges at cell corners.

The energy absorption of structures is generally estimated by integrating the area under the stress-strain curve. Gibson and Ashby [6] present a simplified model for calculating the energy absorption of cellular structures. The small deformation portion is neglected, assuming the curve rises vertically to the final rupture stress. This corresponds to the maximum energy absorption, where the deformation is equal to the densification limit, and the linear-elastic deformation is disregarded. Assuming a nearly constant plateau stress, the maximum energy absorbed per unit volume is given approximately by  $W \approx \sigma_p \varepsilon_D$ . Analytical models relate relative density to energy absorption capacity. An increase in relative density leads to an increase in energy absorption capacity.

### 2.2 Thermal properties

Heat transfer within honeycomb structures is primarily governed by conduction in both solid and gaseous media, with convection and radiation being negligible. When the cell size is small (less than 10 mm), the effect

of natural convection within the cells is minimal. Yang et al. [7] employ the effective thermal conductivity theory, which assumes an ideal homogeneous structure and considers the effective conductivity as a scalar and isotropic value. In this work, the analytical formulation presented by in [7] is used to estimate the effective thermal conductivity, allowing for the simulation of a column protected by the device in a fire scenario. The model formulation demonstrates that, as the relative density of the cellular structure decreases, the effective thermal conductivity value also decreases, thereby enhancing the insulation capacity.

### 3 Formulation and implementation

The proposed protection device enhances structural performance against progressive collapse by focusing on mitigating damage to columns resulting from fires, vehicular collisions, and absorbing energy from slab falls, post-column removal. This device activates during exceptional events, effectively preventing sequential pancake collapses.

The analyzed parking garage has 4 floors, each 3 meters high and 784 square meters in area. The structure includes flat slabs 20 cm thick and columns with dimensions of  $30 \times 30$  cm, reinforced with eight 20 mm diameter steel bars. The concrete has a compressive strength of  $f_{ck} = 30$  MPa, and the steel has a yield strength of  $f_{yk} = 500$  MPa. The device installation involves a 5 cm layer of AA5056 aluminum cellular structure on each column face, with density  $\rho_{Al} = 2700$  kg/m<sup>3</sup>, Young's modulus  $E_{Al} = 70$  GPa, yield stress  $\sigma_{Al} = 435$  MPa. The thermal conductivity is  $\lambda_{Al} = 146.5$  W/(m·°C). In the first meter, the cells are perpendicular to column cross-section, and in the remaining two meters, they align with the cross-section, enhancing vertical compressive strength.

The structural model is analyzed using the Equivalent Frame Method and the Finite Element Method, assuming linear elastic behavior.

The proposed failure sequence for the structural system considers fire and vehicular impact as triggers for the collapse of a central column. Two failure modes are analyzed: a column under flexural-compression during a fire and a column under shear stress due to vehicular impact.

Figure 2 illustrates the failure scenario where the third-floor slabs fail due to column loss in a fire or vehicular impact situation, triggering all the protection devices in that floor. It also includes a perspective view of a protected column.

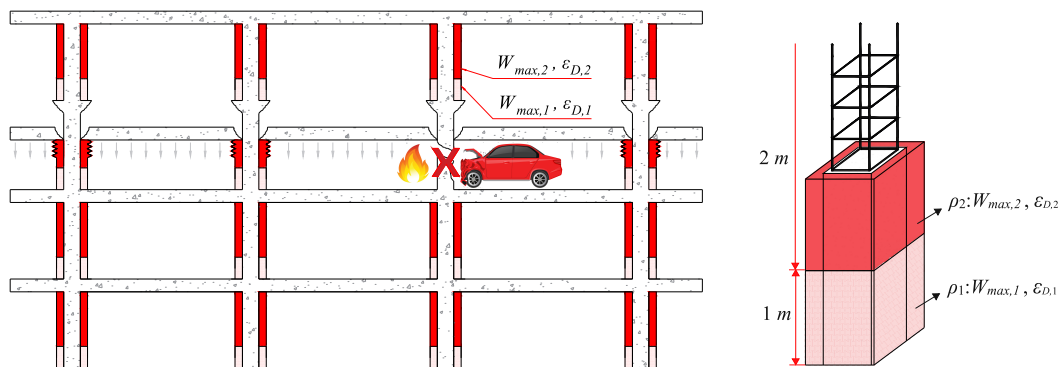


Figure 2. Performance of the device in a collapse situation and perspective view of a protected column.

The initial step in evaluating the column's fire resistance involves conducting a thermal analysis. The column is exposed to a standard "H" hydrocarbon fire curve, which is typical for fires in buildings with significant quantities of flammable materials as parking garages. The Finite Difference Method is employed to solve the Fourier heat conduction equation, which describes heat flow in solids during a transient, two-dimensional analysis. This approach determines the temperature distribution across the column's cross-section when equipped with the protection device. Utilizing the constitutive laws of reinforced concrete at elevated temperatures and the Deformation Compatibility Method, force-moment interaction curves are developed. Ultimately, the limit state equation is derived from the minimum load path criterion, establishing a constant eccentricity limit state, depicted by a linear relationship between axial force and bending moment.

The most common failure mode for columns under vehicular impacts is shear failure. Column shear resistance is estimated using the analytical method outlined in ACI 318-11, which incorporates contributions from compressed concrete and stirrups. To evaluate the shear demand induced by impact, a quasi-static model calculates an equivalent static force on the column based on the vehicle's impact velocity, stiffness, and mass. The honey-

comb protection device acts as a damper by absorbing energy, thereby reducing the vehicle's impact velocity on the column. This reduction subsequently decreases the equivalent static force considered in the calculations.

Two failure modes of the reinforced concrete slabs after the removal of a central column are considered: flexure (positive and negative moments) and punching. For simplicity in analysis and risk optimization, it was assumed that the conditional probability of slab failure, given column loss, on all floors is 1 ( $P[SL|CL, H] = 1$ ), implying that the failure of a single slab could initiate progressive collapse. This conservative assumption, while potentially underestimating slab resistance in extreme conditions, ensures a thorough assessment in the risk optimization process due to the low reliability of flat slabs in such scenarios.

The ultimate failure event, marking the global collapse of the structure, occurs when the protective devices fail under the crushing force from falling slabs. To model the mechanical behavior and describe the failure of these devices, an analytical energy model inspired by Zhou and Yu [8] is adopted. During the progressive pancake-type collapse, the gravitational potential energy of each floor is converted into kinetic energy, accumulated during falls and contributing to the total impact energy. The resistance provided by the lower floors is minimal and insufficient to arrest collapse, as overloaded columns deform slightly before failing, leading to subsequent structural element failures. Therefore, the failure of the protective device is characterized by a limit state equation that evaluates the difference between the energy absorption capacity of devices installed on each floor and the kinetic energy from successive slab falls during collapse.

### 3.1 Risk Optimization

The Genetic Algorithm is employed to find an optimized solution for the risk optimization problem: Determine sets of points  $\mathbf{d}^* = \{\rho_{r,1}^*, \rho_{r,2}^*\}$ , which minimize

$$C_{et}(\mathbf{d}, \mathbf{X}) = C_{device}(\mathbf{d}) + C_{sys}p_{sys}(\mathbf{d}, \mathbf{X}) + C_{CL}p_{CL}(\mathbf{d}, \mathbf{X}), \quad (2a)$$

subject to

$$0,001 \leq \mathbf{d} \leq 0,2. \quad (2b)$$

The design variable  $\rho_{r,1}$  corresponds to the relative density of the first meter of the device, designed to protect against vehicle impacts. Meanwhile,  $\rho_{r,2}$  pertains to the relative density of the remaining length of the device up to the ceiling of the floor, aimed at protecting against slab impacts. The energy absorption capacity of the first meter is also considered, even though the cells are oriented in-plane with the falling slab. The effective thermal diffusivity of the device is determined by  $\rho_{r,2}$ , as this section constitutes the majority of the device's application in the columns, making it more representative. The term  $\mathbf{X}$  represents the random variable vector considered in the reliability analysis. The total expected cost,  $C_{et}$ , is the sum of three terms:

1.  $C_{device}$  denotes the manufacturing cost of the device, estimated based on mass values, assuming a cost of R\$150.00 per kilogram of the fabricated cellular structure. This cost estimation was derived from specific market research for this type of material;
2. Expected cost of system failure ( $C_{sys}$ ) multiplied by the probability of system failure ( $p_{sys}$ ), which addresses the risk associated with structural system failure;
3. Expected cost of local damage ( $C_{CL}$ ) multiplied by the probability of column loss given the hazard occurrence ( $P[CL|H]p_H$ ), which addresses the risk associated with column loss.

The methodology used to establish costs  $C_{sys}$  and  $C_{CL}$  is based on the estimated construction value of the parking garage building. It assumes that  $C_{sys}$  is 40 times the construction cost of the building, and  $C_{CL}$  is 1/4 of the construction cost when  $p_{CL}$  is associated with column failure due to vehicular impact ( $p_{impact}$ ). Conversely,  $C_{sys}$  is 80 times the construction cost of the building, and  $C_{CL}$  is 1/2 of the construction cost when  $p_{CL}$  is related to column failure due to fire ( $p_{fire}$ ). This differentiation is based on the severe consequences that fires can cause, such as panic situations, fire spread to adjacent buildings, structural compromise due to high temperatures, among others. The adopted cost factors reflect the expected costs of failure according to studies conducted by Beck et al. [9].

The estimated total construction cost for the building is approximately R\$4,500,000. This amount is derived from unit costs of concrete and steel, as well as costs related to preliminary services, infrastructure, and complementary items such as installations. The SINAPI database was used to estimate the total construction cost in Brazilian Real, based on unencumbered prices for São Paulo as of November 2023.

### 3.2 Reliability analysis

The First Order Reliability Method (FORM) is utilized in this study to estimate the failure probabilities  $p_f$ , which are necessary for computing  $C_{et}$ . In summary, FORM involves mapping and transforming the vector of random variables,  $\mathbf{X}$ , which can have any joint probability distribution  $f_{\mathbf{X}}(\mathbf{x})$  and may be correlated, into a vector of independent standard normal random variables,  $\mathbf{Y}$ , with distribution  $f_{\mathbf{Y}}(\mathbf{y})$ , as presented by Melchers and Beck [1]. FORM addresses problems involving both linear and nonlinear limit state equations by approximating the limit state equation with a hyperplane centered at the design point, approximating the failure domain by a hyperplane at this point. The reliability index  $\beta$  is the minimum distance from the origin of standard normal space to the limit state equation. The uncertainties adopted in this work are presented in Table 1.

Table 1. Uncertainties considered

Variable	Nominal value	Mean	SD	Distribution	Ref.
Concrete resistance ( $f_c$ )	30 MPa	$1,22f_{ck}$	$0,183f_{ck}$	Normal	[10]
Yielding strength ( $f_y$ )	500 MPa	$1,22f_{yk}$	$0,0488f_{yk}$	Normal	[10]
Dead load ( $D_n$ )	25 kN/m <sup>3</sup>	$1,05D_n$	$0,105D_n$	Normal	[4]
Live load in fire situation ( $L_f$ )	2,5 kN/m <sup>2</sup>	$0,24L_f$	$0,156L_f$	Gumbel	[11]
Live load in impact situation ( $L_i$ )	2,5 kN/m <sup>2</sup>	$0,25L_i$	$0,138L_i$	Gamma	[10]
Fire temperature ( $\theta$ )	"H" curve [12] °C	$\theta$	$0,45\theta$	Normal	[13]
Vehicle mass ( $m$ )	2131 kg	$m$	$0,33m$	Normal	[14]
Vehicle speed ( $v$ )	60 km/h	$v$	$0,15v$	Log-normal	[14]

After the installation of the protection device, the structural system includes support columns, flat slabs, and the protection device itself. A potential scenario of progressive collapse involves the sequential failure of all system elements. If an accidental event initially damages a column, the failure sequence of the system can be described in steps, each with an associated occurrence probability: occurrence of the hazard event (fire,  $p_{fire}$ , or vehicular impact,  $p_{impact}$ ):  $p_H \in \{p_{fire}, p_{impact}\}$ ; column loss due to damage from hazard events:  $p_{CL} = \sum_H P[CL|H]p_H$ ; slab loss due to column loss and occurrence of hazard:  $p_{SL} = \sum_H P[SL|CL, H]P[CL|H]p_H$ ; loss of protection devices due to slab collapse:  $p_{sys} = \sum_H P[GC|SL, CL, H]P[SL|CL, H]P[CL|H]p_H$ .

Each event is conditional on the previous one, and the reliability of the structural system is assessed by the probability  $p_{sys}$ . Failure probabilities are computed assuming mutually exclusive events, where the failure of a single column can potentially lead to slab failure. Failure probabilities are converted to reliability indices using the following well-known relationship:  $\beta = \Phi^{-1}[1 - p]$ .

## 4 Results

The selected scenarios for the case studies involve vehicular impacts at average speeds of 60 km/h and fires with temperatures equivalent to the standard H curve, lasting 60 minutes. Probabilities assigned to these events in simulations are  $p_H \in [10^{-1}, 10^{-2}, 10^{-3}, 10^{-4}]$ , resulting in a total of 16 hazard occurrence scenarios. These scenarios aim to evaluate how the economic feasibility of installing the protection device is affected by the severity and frequency of these accidents.

In all analyzed scenarios, the expected failure costs for the building without the protection device are calculated as  $C_{w/o device} = C_{sys}p_{sys}(\mathbf{X}) + C_{CL}p_{CL}(\mathbf{X})$ . This estimation does not consider the device's capability to mitigate slab falls by absorbing kinetic energy. Thus, the system reliability without the device is expressed by  $\beta_{sys w/o device} = \Phi^{-1}[1 - \sum_H P[SL|CL, H]P[CL|H]p_H]$ .

The results depicted in Fig. 3 underscore the significant reduction in expected failure costs achieved by optimal solutions. As lower relative density values improve fire insulation capacity, minimizing this value also reduces the probability of failure in fire scenarios. Thus, the optimization process is primarily governed by configurations that effectively safeguard against vehicular impacts. For scenarios where  $p_{impact} = 10^{-1}$ , the optimal relative densities were found to be  $\{\rho_{r,1}, \rho_{r,2}\} = \{0.1695, 0.001\}$ . This configuration effectively mitigates the probability of column loss due to both types of accidental events, resulting in zero costs associated with local and global failures by minimizing the column loss probability  $P[CL|H]p_H$ .  $C_{et}$  is approximately R\$ 311.5 thousand.

At  $p_{impact} = 10^{-2}$ , a different solution with relative densities near  $\{\rho_{r,1}, \rho_{r,2}\} = \{0.1605, 0.001\}$  resulted in  $C_{et}$  around R\$ 303 thousand. Although this configuration did not completely eliminate costs related to local and

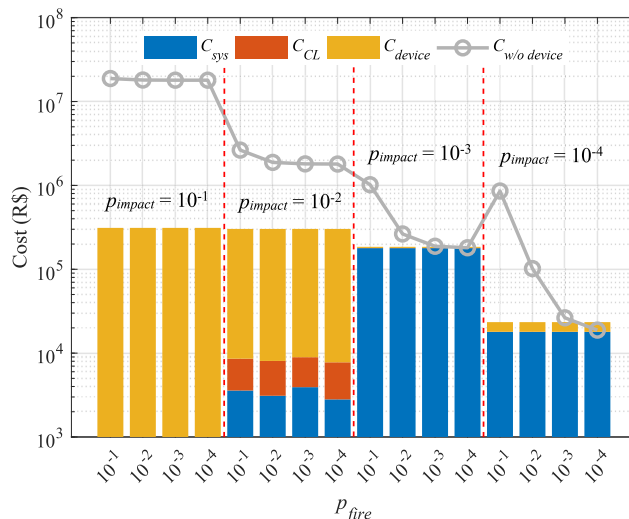


Figure 3. Expected failure costs of the building with and without optimized device.

global failures, it significantly reduced failure costs, particularly concerning system failure. This reduction stems from the first meter's ability to absorb energy from slab impacts, despite being optimized primarily for vehicular impacts. Achieving zero failure costs would necessitate higher densities, pushing manufacturing expenses beyond the optimal threshold identified. Nonetheless, the implemented configuration notably mitigated failure costs in practical scenarios.

The economic feasibility of implementing the device becomes questionable as the occurrence probabilities of accidental events decrease to  $10^{-3}$  and  $10^{-4}$ . Conversely, a reduction in occurrence probability directly correlates with reduced expected costs of failure. In scenarios where both hazard probabilities are very low, the total expected costs of implementing the device exceed those associated with building failures without the device, even with the optimal relative density minimized to  $\{\rho_{r,1}, \rho_{r,2}\} = \{0.001, 0.001\}$  within the solution space.

For a deeper insight into this matter, the reliability indices obtained with optimal solutions for this case are presented in Fig. 4. The results show that increasing the relative density in the first meter of the device effectively enhances column reliability during vehicular collisions and improves the absorption of kinetic energy from slab falls. For  $p_{impact} = 10^{-1}$ , solutions that ensure column integrity are justified. However, at  $p_{impact} = 10^{-2}$ , reliability sharply declines, because optimal configurations tend to prioritize protecting the structure against slab falls rather than preventing column loss. By minimizing manufacturing costs, the relative density of the subsequent two meters of the device is set to its minimum, while energy absorption is warranted by the first meter. Lowering hazard probabilities also contributes to achieving higher reliability levels.

For  $p_{impact} \in \{10^{-3}, 10^{-4}\}$ , reliability indices for the structural system, both with and without the device, nearly converge. This finding highlights that protecting the structure against high-speed vehicular impacts may not be cost-effective for very small impact hazard probabilities. In practical terms, under these conditions, the implementation cost of the device may outweigh the potential savings from reduced expected failure costs.

## 5 Conclusions

Risk optimization shows that the economic feasibility of installing the protective device depends on the probability of hazard occurrence. Highly vulnerable buildings with high failure costs justify protection methods, especially those that mitigate initial damage and avoid repair costs from element loss. As the probability of hazard occurrence decreases, the device may become impractical if its costs exceed the expected reduction in collapse costs.

From a practical perspective, the device can be particularly effective in parking garages with flat slabs, where the absence of beams or capitals makes the direct connection to columns vulnerable to critical failures. The device's versatility is significant in preventing progressive collapse. It not only mitigates initial column damage but also controls collapse propagation through energy absorption from falling slabs, including pancake collapses, a phenomenon still underexplored in the literature but of great practical relevance for structural safety. The optimization explores scenarios where the solution either prioritizes preventing local element failure or opts for a configuration that, while not guaranteeing high protection against accidental events, controls slab failure propagation.

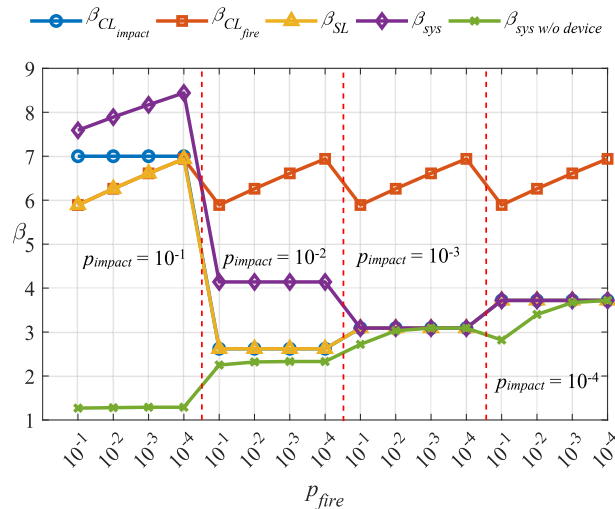


Figure 4. Reliability indices of the building with and without the optimized device.

**Acknowledgements.** Funding of this research project by Brazilian agencies CAPES (Brazilian Higher Education Council) and CNPq (Brazilian National Council for Research, grant n. 306373/2016-5).

**Authorship statement.** The authors hereby confirm that they are the sole liable persons responsible for the authorship of this work, and that all material that has been herein included as part of the present paper is either the property (and authorship) of the authors, or has the permission of the owners to be included here.

## References

- [1] R. E. Melchers and A. T. Beck. *Structural reliability analysis and prediction*. John Wiley & Sons, 2018.
- [2] F. Kiakojour, V. Biagi, B. Chiaia, and M. R. Sheidaii. Strengthening and retrofitting techniques to mitigate progressive collapse: A critical review and future research agenda. *Engineering Structures*, vol. 262, pp. 114274, 2022.
- [3] A. T. Beck, L. d. R. Ribeiro, and M. Valdebenito. Cost-benefit analysis of design for progressive collapse under accidental or malevolent extreme events. pp. 313–334. Springer, 2022.
- [4] D. O. Ellingwood. Building design for abnormal loads and progressive collapse. *Computer-Aided Civil and Infrastructure Engineering*, vol. 20, n. 3, pp. 194–205, 2005.
- [5] Z. Wang. Recent advances in novel metallic honeycomb structure. *Composites Part B: Engineering*, vol. 166, pp. 731–741, 2019.
- [6] L. Gibson and M. Ashby. *Cellular Solids: Structure and Properties*. Cambridge University Press, Cambridge, 2nd edition, 1997.
- [7] X. Yang, T. Lu, and T. Kim. Effective thermal conductivity modelling for closed-cell porous media with analytical shape factors. *Transport in porous media*, vol. 100, pp. 211–224, 2013.
- [8] Q. Zhou and T. Yu. Use of high-efficiency energy absorbing device to arrest progressive collapse of tall building. *Journal of Engineering Mechanics*, vol. 130, n. 10, pp. 1177–1187, 2004.
- [9] A. T. Beck, L. d. R. Ribeiro, and M. Valdebenito. Risk-based cost-benefit analysis of frame structures considering progressive collapse under column removal scenarios. *Engineering Structures*, vol. 225, pp. 111295, 2020.
- [10] W. C. Santiago, H. M. Kroetz, S. H. d. C. Santos, F. R. Stucchi, and A. T. Beck. Reliability-based calibration of main Brazilian structural design codes. *Latin American Journal of Solids and Structures*, vol. 17, 2020.
- [11] A. S. Nowak and M. M. Szerszen. Calibration of design code for buildings (aci 318): Part 1—statistical models for resistance. *Structural Journal*, vol. 100, n. 3, pp. 377–382, 2003.
- [12] Eurocode. Design of concrete structures 1-2: General rules-structural fire design (en 1992-1-2), 2004.
- [13] C. D. Eamon and E. Jensen. Reliability analysis of reinforced concrete columns exposed to fire. *Fire safety journal*, vol. 62, pp. 221–229, 2013.
- [14] R. Thomas, K. Steel, and A. D. Sorensen. Reliability analysis of circular reinforced concrete columns subject to sequential vehicular impact and blast loading. *Engineering Structures*, vol. 168, pp. 838–851, 2018.